

LGBQPC: Local Granular-Ball Quality Peaks Clustering

Zihang Jia, Zhen Zhang, *Senior Member, IEEE* and Witold Pedrycz, *Life Fellow, IEEE*

Abstract—The density peaks clustering (DPC) algorithm has attracted considerable attention for its ability to detect arbitrarily shaped clusters based on a simple yet effective assumption. Recent advancements integrating granular-ball (GB) computing with DPC have led to the GB-based DPC (GBDPC) algorithm, which improves computational efficiency. However, GBDPC demonstrates limitations when handling complex clustering tasks, particularly those involving data with complex manifold structures or non-uniform density distributions. To overcome these challenges, this paper proposes the local GB quality peaks clustering (LGBQPC) algorithm, which offers comprehensive improvements to GBDPC in both GB generation and clustering processes based on the principle of justifiable granularity (POJG). Firstly, an improved GB generation method, termed GB-POJG+, is developed, which systematically refines the original GB-POJG in four key aspects: the objective function, termination criterion for GB division, definition of abnormal GB, and granularity level adaptation strategy. GB-POJG+ simplifies parameter configuration by requiring only a single penalty coefficient and ensures high-quality GB generation while maintaining the number of generated GBs within an acceptable range. In the clustering phase, two key innovations are introduced based on the GB k -nearest neighbor graph: relative GB quality for density estimation and geodesic distance for GB distance metric. These modifications substantially improve the performance of GBDPC on datasets with complex manifold structures or non-uniform density distributions. Extensive numerical experiments on 40 benchmark datasets, including both synthetic and publicly available datasets, validate the superior performance of the proposed LGBQPC algorithm.

Index Terms—Clustering, granular computing, granular-ball, density peaks clustering, k -nearest neighbor graph, principle of justifiable granularity.

I. INTRODUCTION

CLUSTERING analysis is a fundamental task in unsupervised machine learning [1], aiming to uncover inherent patterns and structures within data distributions without relying on instance labels. In this context, a cluster represents a group of instances exhibiting higher similarity to each other than to those in other clusters. Over the past few decades, numerous

This work was partly supported by the National Natural Science Foundation of China under Grant Nos. 72371049 and 71971039, the Natural Science Foundation of Liaoning Province under Grant No. 2024-MSBA-26 and the Funds for Humanities and Social Sciences of Ministry of Education of China under Grant No. 23YJC630219. (*Corresponding author: Zhen Zhang.*)

Zihang Jia and Zhen Zhang are with the Institute of Systems Engineering, School of Economics and Management, Dalian University of Technology, Dalian 116024, China (e-mails: zihangjia@outlook.com; zhen.zhang@dlut.edu.cn).

Witold Pedrycz is with the Department of Measurement and Control Systems, Silesian University of Technology (SUT), 44-100 Gliwice, Poland, also with the Department of Electrical and Computer Engineering, University of Alberta, Edmonton, AB T6G 2R3, Canada, also with the Institute of Systems Engineering, Macau University of Science and Technology, Macau, China, and also with the Research Center of Performance and Productivity Analysis, Istinye University, 34010 Istanbul, Türkiye (e-mail: wpedrycz@ualberta.ca).

clustering algorithms have been developed to tackle diverse tasks, such as k -means clustering [2], spectral clustering (SC) [3], density-based spatial clustering of applications with noise (DBSCAN) [4], and density peaks clustering (DPC) [5].

Among these algorithms, DPC has attracted considerable attention due to its straightforward assumptions and capability to identify clusters with arbitrary shapes [6]. Specifically, DPC operates on two fundamental premises: (1) a cluster center exhibits a higher density than its neighbors, and (2) it maintains a relatively large distance from any instance with a higher density. Following the identification of cluster centers, non-center instances are assigned to cluster centers according to their nearest neighbor with higher density. Nevertheless, DPC has a time and space complexity of $O(n^2)$, where n denotes the number of instances, thereby limiting its applicability to large datasets. Research efforts have been directed toward addressing various challenges associated with DPC, such as clustering data with non-uniform density [7], handling large-scale data [8], clustering imbalanced data [9], developing parameter-free algorithms [10], clustering data with complex manifold structures [11], and clustering heterogeneous data [12].

Recently, to enhance the efficiency and robustness of clustering results, Cheng et al. [13] developed an improved DPC algorithm by integrating granular-ball (GB) computing, resulting in the GB-based DPC (GBDPC) algorithm. GB computing, initially introduced by Xia et al. [14], is an efficient, robust, and interpretable computing paradigm. Within this paradigm, GBs with multiple granularities are efficiently generated from instances with single granularity and serve as the fundamental computing units. Notably, the number of generated GBs is considerably lower than that of the original instances, thereby significantly enhancing computational efficiency. Consequently, the GBDPC algorithm necessitates only the calculation of the density of each GB and the distances between GBs, without depending on the finest-grained instances, thus achieving robust clustering results efficiently. Based on the GB computing paradigm, several GB-based clustering algorithms have been developed, including GB-based spectral clustering (GBSC) [15], GB-based DBSCAN (GB-DBSCAN) [16], GBCT [17], GB-FuzzyStream for stream clustering [18], and W-GBC for high-dimensional data clustering [19].

However, GBDPC demonstrates limitations in effectively handling complex clustering tasks, particularly those involving datasets with non-uniform density distribution or complex manifolds. These limitations can be attributed to the following factors:

- (1) The performance of GBDPC heavily relies on the quality of the generated GBs. To address this, based on the principle of justifiable granularity (POJG), Jia et al. [20] developed GB-POJG, an advanced GB generation

method specifically designed for clustering tasks. While GB-POJG have significantly enhanced the performance of GBDPC, it demonstrates two inherent limitations: (i) it necessitates the setting of two parameters, and (ii) it cannot generate GBs at a high granularity level while ensuring the number of generated GBs within an acceptable range.

- (2) In the process of GB clustering, GBDPC exhibits two fundamental challenges: (i) its density estimation mechanism overlooks the integration of local structural information for each GB, significantly undermining its performance on datasets with non-uniform density distribution; and (ii) its reliance on Euclidean distance for calculating distance between GBs renders it insufficient to identify complex manifolds.

To address these limitations, this paper aims to develop a novel GB-based clustering algorithm through improving both the GB generation and clustering processes. The main contributions of this paper are summarized as follows:

- (1) To address the inherent limitations of GB-POJG, this paper introduces GB-POJG+, a comprehensive refinement of GB-POJG, focusing on four aspects: objective function, termination criterion for GB division, definition of abnormal GBs, and adaptation strategy for granularity levels. To the best of our knowledge, GB-POJG+ is the only GB generation method that balances the quality and quantity of generated GBs in clustering tasks.
- (2) To effectively cluster data exhibiting non-uniform densities or complex manifolds, a k -nearest neighbor (k -NN) graph is established for the generated GBs. By leveraging the GB k -NN graph, the relative quality is introduced as a density estimator to sufficiently consider local structural information of GBs, while geodesic distance is utilized as the distance metric for GBs to identify complex manifolds.
- (3) Integrating the above contributions, a novel clustering algorithm, termed local GB quality peaks clustering (LGBQPC), is developed to efficiently tackle complex clustering tasks.

The remainder of this paper is structured as follows. Section II presents a thorough review of related works. Section III details the LGBQPC algorithm. Section IV presents a series of numerical experiments to validate the efficacy of the LGBQPC algorithm. Section V summarizes the paper and suggests future research directions.

II. RELATED WORKS

This section reviews foundational concepts and related research on GB computing, GB-POJG and GBDPC. For convenience, the notations used throughout this paper are first introduced as follows. Let $U = \{\mathbf{x}_1, \dots, \mathbf{x}_n\} \subset \mathbb{R}^m$ denote the universe of all instances, where n and m represent the number of instances and features, respectively, and \mathbb{R} is the real domain. The maximum pairwise distance between instances in U is denoted as d_{\max} . For any set X , its cardinality is denoted as $|X|$. Let \mathbf{y} be a vector, then $\|\mathbf{y}\|_2$, $\text{mean}(\mathbf{y})$, $\text{median}(\mathbf{y})$, and $\text{std}(\mathbf{y})$ represent the 2-norm, mean, median and standard deviation of the elements in \mathbf{y} , respectively.

A. Granular-Ball Computing

Granular-ball computing is a computing paradigm consisting of two main steps: (1) generating GBs from the universe, and (2) learning a GB-based model. The formal definition of a GB is as follows.

Definition 1. (See [14], [17]) Let $X \subseteq U$. The GB derived from X is defined as a 4-tuple $\Omega_X = (X, \mathbf{c}_X, R_X^{\text{ave}}, R_X^{\text{max}})$, where $\mathbf{c}_X = (\sum_{\mathbf{x}_i \in X} \mathbf{x}_i) / |X|$, $R_X^{\text{ave}} = (\sum_{\mathbf{x}_i \in X} \|\mathbf{x}_i - \mathbf{c}_X\|_2) / |X|$ and $R_X^{\text{max}} = \max_{\mathbf{x}_i \in X} \|\mathbf{x}_i - \mathbf{c}_X\|_2$ are the center, average radius and maximum radius of Ω_X , respectively. Each $\mathbf{x}_i \in X$ is always considered to belong to Ω_X .

Mathematically, generating GBs involves partitioning the universe into disjoint subsets $\Pi = \{X_1, \dots, X_t\}$ such that instances in each subset X_i are as similar as possible. This yields a corresponding set of GBs, $\Phi = \{\Omega_{X_1}, \dots, \Omega_{X_t}\}$. The learning process of a GB-based model follows the standard model of GB computing, which can be expressed as: $g(\mathbf{x}, \boldsymbol{\theta}) \rightarrow g^*(\Omega_X, \boldsymbol{\theta}^*)$ [21]. Here, $g(\mathbf{x}, \boldsymbol{\theta})$ refers to a traditional instance-driven learning model with a model parameter vector $\boldsymbol{\theta}$, while $g^*(\Omega_X, \boldsymbol{\theta}^*)$ represents a GB-driven learning model with a model parameter vector $\boldsymbol{\theta}^*$. In summary, GB computing improves the model's learning efficiency by efficiently generating GBs and using them as input instead of individual instances. Current research on GB computing primarily focuses on the efficient generation of GBs [20], [22], [23] and their applications to various tasks, such as classification [24], [25], feature selection [26], [27], sampling [28], clustering [13], [15], and outlier detection [29], [30].

B. GB-POJG

Generating GBs for clustering tasks is challenging due to the absence of instance labels, which makes evaluating GB quality difficult. The POJG provides a well-established framework for designing and assessing information granules based on their coverage and specificity, without relying on instance labels or any specific formal construct [31], [32]. Building upon the POJG, the GB-POJG approach treats GBs as information granules and defines their coverage and specificity, thus providing a comprehensive assessment of GB quality. Moreover, GB-POJG generates GBs in an unsupervised manner by maximizing the overall quality of the generated GBs, ensuring their alignment with the underlying data distribution.

Definition 2. (See [20]) Let f_1 be an increasing function, and f_2 a decreasing function. The quality level of a GB Ω_X is defined as $\mathcal{Q}(\Omega_X) = \mathcal{Q}_C(\Omega_X) \cdot \mathcal{Q}_S(\Omega_X)$, where $\mathcal{Q}_C(\Omega_X) = f_1(|\{\mathbf{x}_i \in X : \|\mathbf{x}_i - \mathbf{c}_X\|_2 \leq R_X^{\text{ave}}\}|)$ and $\mathcal{Q}_S(\Omega_X) = f_2(R_X^{\text{ave}})$ are the coverage and specificity of Ω_X , respectively.

Remark 1. In [20], the increasing function f_1 and the decreasing function f_2 are specified as $f_1(t) = t$ and $f_2(t) = \exp(-\gamma \cdot t)$, respectively, where $\gamma \geq 0$ is a parameter termed granularity level. Notably, as γ increases, the specificity becomes increasingly significant, thereby encouraging the generation of GBs with smaller average radii. Moreover,

the number of GBs generated by GB-POJG typically increases with the granularity level.

Based on Definition 2, the objective function of GB-POJG is the overall quality of all generated GBs, which can be formally formulated as

$$J(\Phi) = \sum_{i=1}^t \mathcal{Q}(\Omega_{X_i}), \quad (1)$$

where $\Phi = \{\Omega_{X_1}, \dots, \Omega_{X_t}\}$ denotes the set of generated GBs. To maximize the overall quality, GB-POJG follows a top-down paradigm [14] and conducts a pre-division of GBs. To be specific, GB-POJG iteratively divides GBs, commencing from Ω_U , the GB of the entire universe U , to ensure that any GB is derived from instances belonging to the same cluster. This process continues until all GBs are sufficiently small. Notably, the following 2-division method is adopted to divide a given GB Ω_X [21]: let $\mathbf{x}_\alpha = \arg \max_{\mathbf{x}_i \in X} \|\mathbf{x}_i - \mathbf{c}_X\|_2$ and $\mathbf{x}_\beta = \arg \max_{\mathbf{x}_i \in X} \|\mathbf{x}_i - \mathbf{x}_\alpha\|_2$. Then, a GB Ω_X can be divided into GBs Ω_{X_α} and Ω_{X_β} , where

$$X_\alpha = \{\mathbf{x}_i \in X : \|\mathbf{x}_i - \mathbf{x}_\alpha\|_2 \leq \|\mathbf{x}_i - \mathbf{x}_\beta\|_2\}, X_\beta = X/X_\alpha. \quad (2)$$

Throughout the subsequent discussions, GBs Ω_{X_α} and Ω_{X_β} are invariably called sub-GBs of Ω_X . Moreover, in [20], a GB Ω_X is considered sufficiently small, if it holds that $|X| \leq \delta \cdot \sqrt{n}$, where $\delta \in]0, 1]$ is a parameter.

During the pre-division process of GBs, a GB-based binary tree \mathcal{T}_U rooted at GB Ω_U can be naturally established. In tree \mathcal{T}_U , for any GB that is insufficiently small, its sub-GBs, as defined by Eq. (2), are designated as its child nodes. The decision to further divide or retain a node in \mathcal{T}_U as a generated GB is based on its best quality. Moreover, the GBs generated from universe U are determined by calculating the best combination of sub-GBs of GB Ω_U . Specifically, the best quality and the best combination of sub-GBs for a GB are defined as below.

Definition 3. (See [20]) Let \mathcal{T}_U be the GB-based binary tree established by GB-POJG, GB Ω_X be a node in tree \mathcal{T}_U , with sub-GBs Ω_{X_α} and Ω_{X_β} determined by Eq. (2).

- (1) If Ω_X is a non-leaf node, its best quality level $\mathcal{BQ}(\Omega_X)$ is defined as $\mathcal{BQ}(\Omega_X) = \max(\mathcal{Q}(\Omega_X), \mathcal{BQ}(\Omega_{X_\alpha}) + \mathcal{BQ}(\Omega_{X_\beta}))$. Otherwise, $\mathcal{BQ}(\Omega_X) = \mathcal{Q}(\Omega_X)$.
- (2) If it holds that $\mathcal{BQ}(\Omega_X) = \mathcal{Q}(\Omega_X)$, then the best combination of sub-GBs of Ω_X , denoted by $\mathcal{BC}(\Omega_X)$, is given by $\mathcal{BC}(\Omega_X) = \{\Omega_X\}$. Otherwise, $\mathcal{BC}(\Omega_X) = \mathcal{BC}(\Omega_{X_\alpha}) \cup \mathcal{BC}(\Omega_{X_\beta})$.

Since the absence of instance labels may result in some GBs being positioned at decision boundaries or containing noise, potentially resulting in inaccurate decision boundaries, GB-POJG includes a mechanism to detect abnormal GBs. Let $\Phi = \{\Omega_{X_1}, \dots, \Omega_{X_t}\}$ be a set of generated GBs. Table I summarizes three existing criteria for identifying abnormal GBs, where $\mathbf{R}_\Phi^{\text{ave}} = [R_{X_1}^{\text{ave}}, \dots, R_{X_t}^{\text{ave}}]$, $\mathbf{R}_\Phi^{\text{max}} = [R_{X_1}^{\text{max}}, \dots, R_{X_t}^{\text{max}}]$, and $\mathbf{N}_\Phi = [|X_1|, \dots, |X_t|]$. The anomaly detection process iteratively divides abnormal GBs based on a criterion specified in Table I, and this process continues until all abnormal GBs

have been divided.

TABLE I
EXISTING CRITERIA FOR DETECTING ABNORMAL GBs

Reference	Criterion for Detecting Abnormal GBs
[15]	$R_{X_i}^{\text{max}} > 2 \cdot \max(\text{mean}(\mathbf{R}_\Phi^{\text{max}}), \text{median}(\mathbf{R}_\Phi^{\text{max}}))$
[18]	$R_{X_i}^{\text{max}} > 1.5 \cdot \max(\text{mean}(\mathbf{R}_\Phi^{\text{max}}), \text{median}(\mathbf{R}_\Phi^{\text{max}}))$
[20]	$R_{X_i}^{\text{ave}} > 2 \cdot \text{mean}(\mathbf{R}_\Phi^{\text{ave}})$ and $ X_i < 0.5 \cdot \text{mean}(\mathbf{N}_\Phi)$

C. Clustering Granular-Balls Based on Density

In this section, a detailed description of the GBDPC algorithm is provided [13]. GBDPC clusters the generated GBs through the following four main steps [13]: (1) calculating the density of each GB; (2) computing the pairwise distances between GBs; (3) selecting GBs with peak density as cluster centers; (4) assigning each non-center GB to the cluster of its nearest neighbor with higher density. Clearly, the key distinction between GBDPC and the original DPC algorithm lies in the choice of computational units: GBDPC operates on GBs rather than individual data instances. In [13], the density of a GB Ω_X is defined as

$$\rho(\Omega_X) = |X| \cdot \left(R_{X_i}^{\text{ave}} \cdot (R_{X_i}^{\text{max}})^2 \right)^{-1}, \quad (3)$$

while the Euclidean distance between GB centers is employed to measure inter-GB distance. To better capture the geometric characteristics of GBs, an alternative distance metric is adopted in this paper, as shown below:

Definition 4. (See [14]) The distance between two GBs Ω_X and Ω_Y , denoted as $\mathcal{D}(\Omega_X, \Omega_Y)$, is defined as

$$\mathcal{D}(\Omega_X, \Omega_Y) = \max(0, \|\mathbf{c}_X - \mathbf{c}_Y\|_2 - (R_{X_i}^{\text{ave}} + R_{Y_i}^{\text{ave}})). \quad (4)$$

III. DETAILS OF THE LGBQPC ALGORITHM

This section provides a comprehensive description of the proposed LGBQPC algorithm. Specifically, Section III-A introduces an enhanced GB generation method tailored for clustering tasks, referred to as GB-POJG+. Section III-B then presents the GB-based clustering method utilizing the k -NN graph. Finally, the complete LGBQPC algorithm along with its time complexity analysis is detailed in Section III-C.

A. GB-POJG+

This section presents the details of the proposed GB-POJG+ method, which is developed as an enhanced version of GB-POJG. GB-POJG+ incorporates four key enhancements: (1) a revised objective function, (2) a novel termination criterion for GB division, (3) a redefinition of abnormal GBs, and (4) an adaptive strategy for granularity level control.

1) *Objective Function:* The original GB-POJG method is designed to maximize the overall quality of the generated GBs. However, it does not account for the influence of the number of GBs on the subsequent clustering process. In fact, generating too many GBs can degrade computational

efficiency and reduce robustness. To address this issue, a new objective function is proposed for GB-POJG+, formulated as:

$$J^*(\Phi, \lambda) = \left(\sum_{i=1}^t \mathcal{Q}(\Omega_{X_i}) \right) - \lambda t, \quad (5)$$

where $\Phi = \{\Omega_{X_1}, \dots, \Omega_{X_t}\}$ denotes the set of generated GBs, and $\lambda \geq 0$ corresponds the penalty coefficient that regulates the number of generated GBs. This formulation allows for maximizing the overall quality of GBs while keeping their quantity within a reasonable range. Notably, when $\lambda = 0$, Eq. (5) degenerates into the original objective function of GB-POJG (i.e., Eq. (1)).

2) *Termination Criterion for GB Division*: To effectively maximize the revised objective function in Eq. (5), it is imperative to establish a suitable termination criterion for GB division. Rewriting the objective function yields:

$$J^*(\Phi, \lambda) = \sum_{i=1}^t (\mathcal{Q}(\Omega_{X_i}) - \lambda). \quad (6)$$

Here, each term $\mathcal{Q}(\Omega_{X_i}) - \lambda$ can be treated as an individual penalized quality level. Structurally, this form is similar to the original objective in GB-POJG, indicating that similar techniques can be employed for optimization. Consequently, the penalized quality level of a GB can be defined as follows:

Definition 5. Let $\lambda \geq 0$ be a penalty coefficient. The penalized quality level of a GB Ω_X , denoted by $\mathcal{PQ}(\Omega_X, \lambda)$, is defined as $\mathcal{PQ}(\Omega_X, \lambda) = \mathcal{Q}(\Omega_X) - \lambda$, where $\mathcal{Q}(\Omega_X)$ is the quality level of Ω_X defined in Definition 2.

To maximize the objective function Eq. (5), GB-POJG+ adopts a two-stage, parameter-free strategy similar to GB-POJG in its initial stage. This strategy involves GB pre-division and the construction of a binary tree \mathcal{T}_U of GBs, as outlined below:

Step 1: Starting from the initial GB Ω_U derived from the universe U , iteratively divide each GBs until it is sufficiently small, i.e., the number of instances belonging to each GB falls below a threshold $\sqrt[3]{n}$. Subsequently, a binary tree \mathcal{T}_U is then constructed by designating the sub-GBs of each insufficiently small GB as its child nodes.

Step 2: Detect and completely divide abnormal leaf nodes in the tree \mathcal{T}_U established in **Step 1**.

Specifically, both GB-POJG and GB-POJG+ share the common objective of ensuring that each leaf node in \mathcal{T}_U is derived from instances belonging to the same cluster. However, GB-POJG achieves this by enforcing a size threshold (less than $\delta \cdot \sqrt{n}$) for leaf nodes. Although reducing this threshold enables finer division for GBs and better objective attainment, it simultaneously increases the number of GBs generated by GB-POJG [20]. Consequently, to balance clustering efficiency and effectiveness, previous work recommends setting the threshold within $[0.4\sqrt{n}, \sqrt{n}]$ [20]. In contrast, GB-POJG+ avoids over-generation of GBs by directly optimizing its objective function (i.e., Eq. (5)), allowing it to adopt a lower threshold without sacrificing clustering quality. Notably, it holds that $0.4\sqrt{n} > \sqrt[3]{n}$ for $n \geq 245$. This indicates that $\sqrt[3]{n}$ consistently falls below the recommended threshold range for GB-POJG in medium- to large-scale datasets. Hence, GB-POJG+ employs

$\sqrt[3]{n}$ as a parameter-free threshold for the threshold for defining sufficiently small GBs. Furthermore, GB-POJG+ integrates anomaly detection during tree construction to mitigate the adverse of leaf nodes located at decision boundaries or containing noise. Here, the complete division of a GB refers to recursively dividing it until each resulting GB contains only a single instance. Meanwhile, the binary tree \mathcal{T}_U should be updated by designating sub-GBs of each GB as its child nodes.

To further identify which GBs should be retained in the final set, each GB's penalized best quality and penalized best combination of sub-GBs are formally defined in accordance with Definition 3 as follows.

Definition 6. Let \mathcal{T}_U be the binary tree constructed by GB-POJG+, $\lambda \geq 0$ be the penalty coefficient, Ω_X be a node in tree \mathcal{T}_U , $\mathcal{PQ}(\Omega_X, \lambda)$ be the penalized quality level of Ω_X , and Ω_{X_α} and Ω_{X_β} be sub-GBs of Ω_X determined by Eq. (2).

- (1) If Ω_X is a leaf node, its penalized best quality level, denoted by $\mathcal{PBQ}(\Omega_X, \lambda)$, is defined as $\mathcal{PBQ}(\Omega_X, \lambda) = \mathcal{PQ}(\Omega_X, \lambda)$. Otherwise, $\mathcal{PBQ}(\Omega_X, \lambda) = \max(\mathcal{PQ}(\Omega_X, \lambda), \mathcal{PBQ}(\Omega_{X_\alpha}, \lambda) + \mathcal{PBQ}(\Omega_{X_\beta}, \lambda))$.
- (2) If $\mathcal{PBQ}(\Omega_X, \lambda) = \mathcal{PQ}(\Omega_X, \lambda)$, then the penalized best combination of sub-GBs of Ω_X , denoted by $\mathcal{PBC}(\Omega_X, \lambda)$, is $\{\Omega_X\}$. Otherwise, $\mathcal{PBC}(\Omega_X, \lambda) = \mathcal{PBC}(\Omega_{X_\alpha}, \lambda) \cup \mathcal{PBC}(\Omega_{X_\beta}, \lambda)$.

In summary, GB-POJG+ begins by generating an initial set of GBs through a two-stage, parameter-free division process and constructs a binary tree \mathcal{T}_U . Following this, for each GB node in \mathcal{T}_U , if its penalized best quality exceeds its own penalized quality, it is further divided; otherwise, it is retained. Ultimately, the set of generated GBs are determined by the penalized best combination of sub-GBs for the root GB Ω_U .

3) *Definition of Abnormal GBs*: Following previous studies [15], [18], [20], GB-POJG+ iteratively detects and divides anomalies within the generated GBs, thereby improving decision boundary accuracy in subsequent clustering. Notably, the construction of the GB-based binary tree also involves the identification of abnormal GBs. Consequently, the performance of GB-POJG+ heavily depends on the rationality of the abnormal GB definition.

However, as shown in Table I, existing definitions typically consider only either the maximum or average radius of GBs. Moreover, thresholds for identifying abnormal GBs are often based on fixed multiples of the mean or median, making them sensitive to both outliers and data scale. To address these limitations, a refined definition of an abnormal GB is presented as follows.

Definition 7. Let $\Phi = \{\Omega_{X_1}, \dots, \Omega_{X_t}\}$ be a set of GBs, $\mathbf{R}_\Phi^{\text{ave}} = [R_{X_1}^{\text{ave}}, \dots, R_{X_t}^{\text{ave}}]$, $\mathbf{R}_\Phi^{\text{max}} = [R_{X_1}^{\text{max}}, \dots, R_{X_t}^{\text{max}}]$, and $\mathbf{N}_\Phi = [|X_1|, \dots, |X_t|]$. For each $\Omega_{X_i} \in \Phi$ ($i = 1, \dots, t$), it is deemed an abnormal GB, if one of the following conditions is met: (1) $R_{X_i}^{\text{max}} > \text{mean}(\mathbf{R}_\Phi^{\text{max}}) + \text{std}(\mathbf{R}_\Phi^{\text{max}})$; (2) $R_{X_i}^{\text{ave}} > \text{mean}(\mathbf{R}_\Phi^{\text{ave}}) + \text{std}(\mathbf{R}_\Phi^{\text{ave}})$ and $|X_i| < \text{mean}(\mathbf{N}_\Phi) - \text{std}(\mathbf{N}_\Phi)$.

Remark 2. Definition 7 introduces a more comprehensive criterion for identifying abnormal GBs. Specifically, Condition (1), inspired by [15], [18], identifies abnormality based on the maximum radius of a GB, while Condition (2), motivated by

[20], considers both the average radius and the number of instances within a GB. Additionally, by incorporating both the mean and standard deviation, Definition 7 adaptively set thresholds, enhancing robustness in abnormal GB detection. The effectiveness of Definition 7 is further validated through experiments presented in Section IV-D.

4) *Adaptation Strategy for Granularity Level:* GB-POJG+ utilizes the GB quality metric defined in Definition 2. Although this definition offers a comprehensive framework for assessing the quality of GBs, it involves a granularity level parameter that must be carefully tuned to balance coverage and specificity (see Remark 1). To eliminate the need for manual tuning, an adaptive granularity level adjustment strategy is introduced, as detailed below.

The fundamental principle of this strategy is to determine an appropriate granularity level that maximizes the division of GBs satisfying two criteria: (1) the GBs are not sufficiently small, and (2) the instances within them cannot be effectively represented by a hyperspherical structure.

Specifically, in GB-POJG+, most sufficiently small GBs must be retained without further division. Additionally, since the GB computing framework uses hyperspheres to represent instance distributions, any deviation from this assumption may misalign the resulting GBs with the actual data distribution. Consider the synthetic datasets shown in Figs. 1(a)-(c). Clearly, the instances shown in Fig. 1(a) are well-represented by a hypersphere. In contrast, those in Figs. 1(b) and 1(c) exhibit significant limitations for such representation due to significant variation in feature dispersion and strong feature correlation, respectively. In GB-POJG+, feature dispersion is quantified by the coefficient of variation in feature variances, while feature correlation is measured by the absolute value of the correlation coefficient. According to empirical experience, a coefficient of variation below 0.1 indicates low dispersion [33], and a correlation coefficient below 0.3 indicates a relatively weak inter-feature correlation [34]. These criteria guide the formal definition below.

Definition 8. A GB Ω_X is said to satisfy the granularity level adjustment criterion, if (1) $|X| \geq \sqrt[3]{n}$, and (2) the instances within Ω_X exhibit either a coefficient of variation in feature variances exceeding 0.1 or an absolute correlation coefficient between features greater than 0.3.

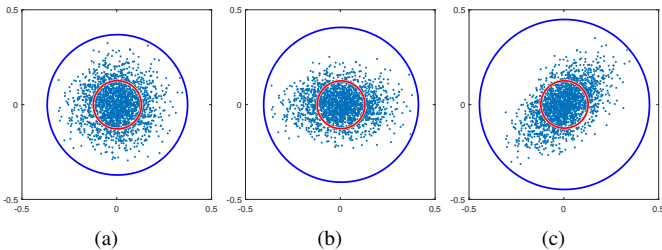


Fig. 1. Three GBs with average (red) and maximum (blue) radii.

Furthermore, according to Definition 6, any non-leaf node

in the tree \mathcal{T}_U must be divided, if it satisfies:

$$\begin{aligned} \mathcal{PQ}(\Omega_X, \lambda) &< \mathcal{PQ}(\Omega_{X_\alpha}, \lambda) + \mathcal{PQ}(\Omega_{X_\beta}, \lambda) \\ &\leq \mathcal{PBQ}(\Omega_{X_\alpha}, \lambda) + \mathcal{PBQ}(\Omega_{X_\beta}, \lambda). \end{aligned} \quad (7)$$

In conjunction with Definitions 2, 5, and 6, and Remark 1, Eq. (7) can be reformulated as:

$$\frac{\mathcal{Q}_C(\Omega_X)}{\exp(\gamma \cdot R_X^{\text{ave}})} < \frac{\mathcal{Q}_C(\Omega_{X_\alpha})}{\exp(\gamma \cdot R_{X_\alpha}^{\text{ave}})} + \frac{\mathcal{Q}_C(\Omega_{X_\beta})}{\exp(\gamma \cdot R_{X_\beta}^{\text{ave}})} - \lambda. \quad (8)$$

Since Eq. (8) is a transcendental inequality in terms of the granularity level γ and typically lacks an analytical solution, this paper adopts the following approximations as in Definition 2:

$$f_1(t) = t \text{ and } f_2(t) = (1 + \gamma \cdot t)^{-1}. \quad (9)$$

Substituting these into Eq. (7) yields:

$$\frac{\mathcal{Q}_C(\Omega_X)}{1 + \gamma \cdot R_X^{\text{max}}} < \frac{\mathcal{Q}_C(\Omega_{X_\alpha})}{1 + \gamma \cdot R_{X_\alpha}^{\text{max}}} + \frac{\mathcal{Q}_C(\Omega_{X_\beta})}{1 + \gamma \cdot R_{X_\beta}^{\text{max}}} - \lambda, \quad (10)$$

which is a tractable cubic inequality that permits analytical solutions. Following the global-first cognitive mechanism [35], the adaptation strategy prioritizes GBs encountered earlier in the pre-division stage. Consequently, the full strategy is described below:

Step 1: Initialize the granularity level range as $\bar{\gamma} = [0, +\infty[$.

Step 2: Perform a breadth-first search starting from the root node of the GB-based binary tree established by GB-POJG+. For each GB encountered during the search that satisfies the granularity level adjustment criterion in Definition 8, solve Eq. (10) to determine the solution set γ^* . Whenever $\bar{\gamma} \cap \gamma^* \neq \emptyset$, update $\bar{\gamma}$ to $\bar{\gamma} \cap \gamma^*$.

Step 3: Set the granularity level γ as $\gamma = \inf_{\theta \in \bar{\gamma}} \theta + \varepsilon$, where ε is a sufficiently small positive constant.

B. Clustering Granular-Balls Based on Local Quality Peaks

In GBDPC, the GB density is calculated using Eq. (3), which exhibits two critical limitations: (1) GBs composed of only a few closely clustered noise instances may be assigned excessively high density values, and (2) GB density is estimated from a global perspective, disregarding local neighborhood information. These shortcomings can result in erroneous clustering results, particularly on datasets with non-uniform density distributions. Moreover, GBDPC measures the distance between GBs using the Euclidean distance between their centers, which fails to capture the geometric structure of GBs and identify complex manifold structures. To overcome these limitations and further enhance the performance of GBDPC, this section redefines both the density estimation and distance metrics for GBs.

To begin with, a new method for density estimation is proposed. As shown in Definition 2 and Eq. (3), both GB quality and density are positively correlated with the number of instances within the GB and negatively correlated with its radius. Moreover, the GB quality, as specified by Definition

Algorithm 1: LGBQPC

Input : Universe $U = \{\mathbf{x}_1, \dots, \mathbf{x}_n\}$, number of clusters c , penalty coefficient λ , and number of neighbors k .
Output: Set of instance labels $\mathcal{L} = \{\mathcal{L}(\mathbf{x}_1), \dots, \mathcal{L}(\mathbf{x}_n)\}$.

- 1 **Initialize**: a tree \mathcal{T}_U rooted at the GB Ω_U , granularity level range $\bar{\gamma} \leftarrow [0, +\infty[$, and a sufficiently small positive constant ε .
 /* Initial GB generation using GB-POJG+ */
- 2 **while** $\exists \Omega_X \in \mathcal{T}_U$ such that $|X| > \bar{\gamma}n$, and Ω_X is a leaf node **do**
 - 3 // perform breadth-first search
 - 4 divide Ω_X into Ω_{X_α} and Ω_{X_β} using Eq. (2);
 - 5 designate Ω_X as the parent node of Ω_{X_α} and Ω_{X_β} ;
 - 6 **if** Ω_X satisfies the granularity level adjustment criterion in Definition 8 **then**
 - 7 $\gamma^* \leftarrow$ the solution to Eq. (10) for Ω_X ;
 - 8 **if** $\bar{\gamma} \cap \gamma^* \neq \emptyset$ **then**
 - 9 $\bar{\gamma} \leftarrow \bar{\gamma} \cap \gamma^*$;
- 9 $\gamma \leftarrow \inf_{\theta \in \bar{\gamma}} \theta + \varepsilon$; // obtain granularity level
- 10 detect abnormal GBs among all leaf nodes in \mathcal{T}_U using Definition 7;
- 11 **foreach** leaf node $\Omega_X \in \mathcal{T}_U$ **do**
 - 12 **if** Ω_X is abnormal **then**
 - 13 fully divide Ω_X using Eq. (2) and update \mathcal{T}_U ;
- 14 **foreach** $\Omega_X \in \mathcal{T}_U$ **do**
 - 15 calculate $\mathcal{PBQ}(\Omega_X)$ and $\mathcal{PBC}(\Omega_X)$ by Definition 6;
 - 16 $\Phi \leftarrow \mathcal{PBC}(\Omega_U)$;
 - 17 detect abnormal GBs in Φ using Definition 7;
 - 18 **while** $\exists \Omega_X \in \Phi$ is abnormal **do**
 - 19 $\Phi \leftarrow (\Phi / \{\Omega_X\}) \cup \{\Omega_{X_\alpha}, \Omega_{X_\beta}\}$ using Eq. (2);
 - /* Clustering based on the GB k -NN graph */
 - 20 construct the GB k -NN graph $\mathcal{G}_k = (\Phi, \mathcal{E})$ by Definition 9;
 - 21 calculate the relative quality for each $\Omega_X \in \Phi$ using Definition 10;
 - 22 calculate the geodesic distance between each pair of GBs in Φ using Definition 11; // using Dijkstra's algorithm
 - 23 calculate the relative geodesic distance and relative nearest neighbor for each $\Omega_X \in \Phi$ using Definition 12;
 - 24 calculate the decision value for each $\Omega_X \in \Phi$ using Definition 13;
 - 25 sort all GBs in Φ in descending order of decision values, resulting in the ordered set $\Phi = \{\Omega_{X_{i_1}}, \dots, \Omega_{X_{i_p}}\}$;
 - 26 **for** $j = 1$ to p **do**
 - 27 **if** $1 \leq j \leq c$ **then**
 - 28 $\mathcal{L}_{GB}(\Omega_{X_{i_j}}) \leftarrow j$;
 - 29 **else**
 - 30 $\mathcal{L}_{GB}(\Omega_{X_{i_j}}) \leftarrow \mathcal{L}_{GB}(\mathcal{N}_R(\Omega_{X_{i_j}}))$;
 - 31 **foreach** $\mathbf{x}_q \in X_{i_j}$ **do**
 - 32 $\mathcal{L}(\mathbf{x}_q) \leftarrow \mathcal{L}_{GB}(\Omega_{X_{i_j}})$;
 - 33 **return**: the set of instance labels $\mathcal{L} = \{\mathcal{L}(\mathbf{x}_1), \dots, \mathcal{L}(\mathbf{x}_n)\}$;

2 and Eq. (9), is bounded within the interval $]0, \mathcal{Q}_C(\Omega_X)]$. These findings imply that utilizing this quality metric for GB density estimation can effectively avoid overestimating density. Additionally, inspired by [7], a cluster center is required to exhibit only locally higher density compared to its neighbors rather than globally. Accordingly, to handle non-uniform density distributions more effectively, a relative quality metric is introduced for GB density estimation, incorporating both the GB quality metric and neighborhood information. This is achieved by constructing a GB k -NN graph for the generated GBs, as defined below.

Definition 9. A GB k -NN graph is defined as a 2-tuple $\mathcal{G}_k = (\Phi, \mathcal{E})$, where $\Phi = \{\Omega_{X_1}, \dots, \Omega_{X_t}\}$ is the set of GBs, and an edge $(\Omega_{X_i}, \Omega_{X_j}) \in \mathcal{E}$ exists if and only if Ω_{X_j} is among the k nearest neighbors of Ω_{X_i} according to the distance metric

defined in Eq. (4).

Based on Definition 9, the relative quality metric for a GB is defined as follows.

Definition 10. Let $\mathcal{G}_k = (\Phi, \mathcal{E})$ be a GB k -NN graph. For any $\Omega_{X_i} \in \Phi$, its relative quality $\mathcal{RQ}(\Omega_{X_i})$ is defined as

$$\mathcal{RQ}(\Omega_{X_i}) = \frac{\mathcal{Q}(\Omega_{X_i})}{\frac{1}{k} \sum_{(\Omega_{X_i}, \Omega_{X_j}) \in \mathcal{E}} \mathcal{Q}(\Omega_{X_j})}. \quad (11)$$

Next, a new distance metric for GBs is introduced to further enhance GBDPC. According to [11], the geodesic distance between instances demonstrates superiority in identifying complex manifold structures and improving DPC performance. Building on this idea, Eq. (4), which is capable of capturing the geometric structure of GBs, is extended to define the geodesic distance between GBs over the GB k -NN graph.

Definition 11. Let $\mathcal{G}_k = (\Phi, \mathcal{E})$ be a GB k -NN graph. For any pair $\Omega_{X_i}, \Omega_{X_j} \in \Phi$, the geodesic distance $\mathcal{D}_G(\Omega_{X_i}, \Omega_{X_j})$ is the length of the shortest path between them on \mathcal{G}_k .

With newly defined density and distance metrics, the criteria for identifying cluster centers and assigning non-center GBs are accordingly refined. To support this refinement, two key concepts are introduced: the relative geodesic distance, which assesses the minimum distance from a GB to any GB with higher relative quality, and the relative nearest neighbor, which identifies the nearest GB with higher relative quality.

Definition 12. Let $\mathcal{G}_k = (\Phi, \mathcal{E})$ and $\Omega_{X_i} \in \Phi$. Define the set of GBs with higher relative quality than Ω_{X_i} as $\mathcal{Y}(\Omega_{X_i}) = \{\Omega_{X_j} \in \Phi : \mathcal{RQ}(\Omega_{X_j}) > \mathcal{RQ}(\Omega_{X_i})\}$. The relative geodesic distance of Ω_{X_i} , denoted by $\mathcal{D}_{RG}(\Omega_{X_i})$, is defined as

$$\mathcal{D}_{RG}(\Omega_{X_i}) = \begin{cases} \max_{\Omega_{X_j} \in \Phi} \mathcal{D}_G(\Omega_{X_i}, \Omega_{X_j}), & \text{if } \mathcal{Y}(\Omega_{X_i}) = \emptyset, \\ \min_{\Omega_{X_j} \in \mathcal{Y}(\Omega_{X_i})} \mathcal{D}_G(\Omega_{X_i}, \Omega_{X_j}), & \text{otherwise.} \end{cases} \quad (12)$$

Furthermore, the relative nearest neighbor of Ω_{X_i} , denoted by $\mathcal{N}_R(\Omega_{X_i})$, is defined as

$$\mathcal{N}_R(\Omega_{X_i}) = \begin{cases} \Omega_{X_i}, & \text{if } \mathcal{Y}(\Omega_{X_i}) = \emptyset, \\ \arg \min_{\Omega_{X_j} \in \mathcal{Y}(\Omega_{X_i})} \mathcal{D}_G(\Omega_{X_i}, \Omega_{X_j}), & \text{otherwise.} \end{cases} \quad (13)$$

Following the GBDPC framework [13] and based on Definition 12, the following refinements are implemented for cluster center identification and non-center GB label assignment:

- A GB is designated as a cluster center (or local quality peak), if it possesses both high relative quality and a large relative geodesic distance.
- A non-center GB inherits the cluster label of its relative nearest neighbor.

To automate the selection of cluster centers and eliminate manual intervention, a decision value similar to that proposed in [5] is introduced. GBs are ranked in descending order of their decision values, and the top-ranking GBs are designated as cluster centers.

Definition 13. Let $\mathcal{G}_k = (\Phi, \mathcal{E})$ be a GB k -NN graph. The decision value of GB $\Omega_{X_i} \in \Phi$ is defined as

$$DV(\Omega_{X_i}) = \mathcal{RQ}(\Omega_{X_i}) \cdot \mathcal{D}_{RG}(\Omega_{X_i}), \quad (14)$$

where $\mathcal{RQ}(\Omega_{X_i})$ and $\mathcal{D}_{RG}(\Omega_{X_i})$ are determined by Eqs. (11) and (12), respectively.

C. The LGBQPC Algorithm and Its Time Complexity Analysis

The proposed LGBQPC algorithm is outlined in Algorithm 1. It consists of two key components: (1) the generation of GBs using GB-POJG+ and (2) the clustering of the resulting GBs based on the GB k -NN graph. An illustrative example of the clustering process is provided in Fig. 2.

The time complexity of Algorithm 1 is analyzed as follows. Let k be the number of neighbors in the GB k -NN graph, t be the number of leaf nodes in the tree \mathcal{T}_U obtained after the execution of line 8, and p denote the number of GBs generated after executing line 19. If \mathcal{T}_U is a full binary tree, the time complexity of lines 2-8 is $O(n \log(t))$, representing the best-case scenario. In contrast, the worst-case time complexity occurs when each left (or right) child node contains only a single instance, leading to a complexity of approximately $O(n^2)$. According to [20], the operations in lines 9-19, which involve abnormal GB detection and penalized quality evaluation, incur a time complexity of approximately $O(t)$. Line 20 constructs the GB k -NN graph over p GBs, requiring a complexity of $O(p^2 + kp^2)$. Line 21 calculates the relative quality for each GB based on its k nearest neighbors, which takes $O(pk)$ time. Line 22 employs Dijkstra's algorithm to calculate the shortest path between all pairs of GBs, resulting in a complexity of $O(kp^2 \log p)$. Line 23, which ranks the GBs by their decision values, has a complexity of $O(p \log p + p^2)$. Finally, lines 24-32 perform the final labeling based on GBs and instances, with an overall complexity of $O(p + p \log p + n)$. In summary, the overall time complexity of Algorithm 1 is approximately $O(n \log t + kp^2 \log p)$ in the best case. In the worst case, the complexity increases to approximately $O(n^2 + kp^2 \log p)$.

IV. NUMERICAL EXPERIMENTS

This section presents extensive numerical experiments to validate the performance of LGBQPC.

A. Experimental Setups

1) *Experimental Environment:* All experiments are conducted on a workstation running MATLAB 2024b, with system specifications comprising an Intel Core i9-13900HX CPU, 32.0 GB of RAM, and Windows 11 operating system.

2) *Datasets:* This study employs a total of 40 datasets, comprising 27 synthetic datasets and 13 publicly available datasets, as detailed in Table II. The synthetic datasets are adopted to evaluate the algorithms' ability to cluster data with complex and arbitrary shapes, while the publicly available datasets are used to evaluate their practical applicability. Prior to experimentation, all features are standardized to have zero mean and unit variance to ensure uniformity in scale across all features.

TABLE II
INFORMATION OF DATASETS

ID	Dataset	Source	#Instances	#Features	#Clusters	Type
D1	Flame	[6]	240	2	2	S
D2	Zelink3	[6]	266	2	3	S
D3	Zelink1	[6]	299	2	3	S
D4	Spiral	[6]	312	2	3	S
D5	Jain	[6]	373	2	2	S
D6	2circles	[6]	600	2	2	S
D7	2d-3c-no123	[6]	715	2	3	S
D8	Atom	[6]	800	3	2	S
D9	2d-4c-no4	[6]	863	2	4	S
D10	Donut3	[6]	999	2	3	S
D11	Chainlink	[6]	1000	3	2	S
D12	Smile2	[6]	1000	2	4	S
D13	Pearl	[6]	1000	2	2	S
D14	Halfkernel	[6]	1000	2	2	S
D15	Donutcurves	[6]	1000	2	4	S
D16	Dartboard2	[6]	1000	2	4	S
D17	Dartboard1	[6]	1000	2	4	S
D18	Curves2	[6]	1000	2	2	S
D19	Crossline	[6]	1000	2	2	S
D20	Crescentfullmoon	[6]	1000	2	2	S
D21	2spiral	[6]	1000	2	2	S
D22	Clusterincluster	[6]	1012	2	2	S
D23	Complex9	[6]	3031	2	9	S
D24	Banana	[6]	4811	2	2	S
D25	Algerian Forest Fires (Bejaia)	[36]	122	13	2	PA
D26	Algerian Forest Fires (Sidi-Bel Abbas)	[36]	122	13	2	PA
D27	Iris	[36]	150	4	3	PA
D28	Planning Relax	[36]	182	12	2	PA
D29	Wpbc	[36]	194	32	2	PA
D30	Glass Identification	[36]	214	9	6	PA
D31	Speaker Accent Recognition	[36]	329	12	6	PA
D32	Wholesale Customers	[36]	440	7	3	PA
D33	Blood Transfusion Service Center	[36]	748	4	2	PA
D34	Iranian Churn	[36]	3150	13	2	PA
D35	Abalone	[36]	4177	8	3	PA
D36	Electrical Grid	[36]	10000	13	2	PA
D37	Synthetic Circle	[36]	10000	2	100	S
D38	MAGIC Gamma Telescope	[36]	19020	10	2	PA
D39	TB-60K	[37]	60000	2	2	S
D40	CC-60K	[37]	60000	2	3	S

Note: "S" and "PA" represent synthetic and publicly available, respectively.

3) *Baseline Algorithms and Parameter Settings:* To demonstrate the superiority of LGBQPC, it is compared against eleven well-established clustering algorithms: k-means++ [2], SC [3], DBSCAN [4], DPC [5], DPC-DLP [38], FHC-LDP [39], USPEC [37], USENC [37], GBDPC [13], GBSC [15], and GBCT [17]. The parameters for each algorithm are configured as follows:

- For SC and GBSC, the affinity matrix is constructed using a k -NN graph, where $k = \lfloor \log_2 n \rfloor + 1$ [3].
- For DBSCAN, the neighborhood radius is searched within $d_{\max} \cdot \{0, 0.01, \dots, 0.3\}$, with the minimum number of neighbors required for core points set to $2m$ [40].
- For DPC, the truncation distance is selected within $d_{\max} \cdot \{0.02, 0.04, \dots, 0.5\}$.
- For DPC-DLP, the local density parameter is varied within $\{0.1, 0.2, \dots, 0.5\}$.
- For FHC-LDP and LGBQPC, the number of nearest neighbors is selected within $\{1, 2, \dots, 20\}$ for datasets D1–D38, and within $\{1, 2, \dots, 30\}$ for datasets D39–D40.
- For LGBQPC, the penalty coefficient is searched within $\sqrt[3]{n} \cdot \{0, 0.01, \dots, 0.3\}$ for datasets D1–D38, and $\sqrt[3]{n} \cdot \{0, 0.005, \dots, 0.2\}$ for datasets D39–D40.

4) *Evaluation Metrics:* To evaluate the performance and efficiency of these clustering algorithm, three widely used metrics, including normalized mutual Information (NMI) [41], adjusted rand index (ARI) [41] and computing overhead (CO) are adopted. Specifically, NMI and ARI fall within the ranges of $[0, 1]$ and $[-1, 1]$, respectively, whereas CO is measured in seconds. Furthermore, higher values of NMI and ARI signifies better clustering performance, whereas lower values of CO

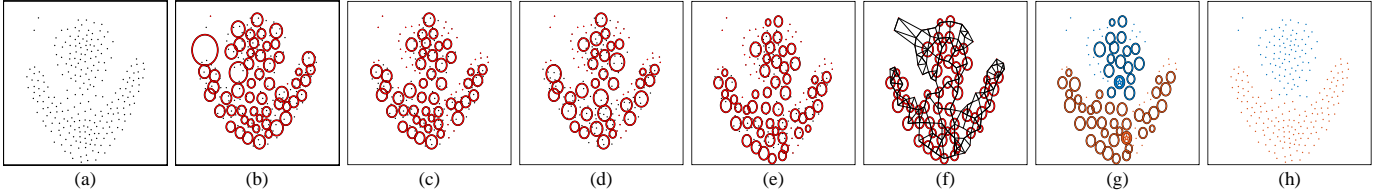


Fig. 2. The LGBQPC clustering process illustrated on the Flame dataset [6]. (a) The original Flame dataset. (b)-(c) GBs serving as leaf nodes in the binary tree: (b) each leaf node is sufficiently small, and (c) each abnormal leaf node has been completely divided. (d) The best combination of sub-GBs of derived from the Flame dataset. (e) GBs generated after applying anomaly detection to those in (d). (f) The GB k -NN graph ($k = 3$). (g) Clustering results at the GB level. (h) Final clustering results at the instance level.

indicates higher clustering efficiency.

5) *Statistical Tests*: To statistically evaluate the performance differences among these algorithms, the Friedman test [42] and Nemenyi test [43] are conducted. The Friedman test begins with computing the statistic τ_F , which follows an F -distribution with degrees of freedom $(N_A - 1)$ and $(N_A - 1)(N_D - 1)$:

$$\tau_F = \frac{(N_D - 1)\tau_{\chi^2}}{N_D(N_A - 1) - \tau_{\chi^2}},$$

$$\tau_{\chi^2} = \frac{12N_D}{N_A(N_A + 1)} \left(\sum_{i=1}^{N_A} r_i^2 - \frac{N_A(N_A + 1)^2}{4} \right).$$

Here, N_A , N_D and r_i denote the number of algorithms being compared, the number of used datasets, and the average rank of i -th algorithm across all datasets. Furthermore, given a significance level η , if τ_F exceeds the critical value $F_{\eta}(N_A - 1, (N_A - 1)(N_D - 1))$, it indicates statistically significant differences among the compared algorithms. Under such circumstances, pairwise differences between the algorithms are subsequently identified using the Nemenyi test. A statistically significant difference is confirmed if the absolute difference between two average ranks exceeds the critical difference $CD_{\eta} = q_{\eta} \sqrt{N_A(N_A + 1)/(6N_D)}$, where q_{η} is the critical value of Tukey's distribution.

B. Experimental Results and Analysis

The experimental results are summarized in Tables III and IV, along with Fig. 3. Specifically, Table III presents the performance of 12 clustering algorithms on the standardized datasets D1-D38, whereas Table IV evaluates nine scalable clustering algorithms on the large-scale datasets D39-D40. Furthermore, Fig. 3 visualizes the clustering results of LGBQPC across all synthetic datasets.

As shown in Table III, LGBQPC demonstrates superior performance compared to the other methods, achieving the highest NMI on 29 datasets and the highest ARI on 28 datasets. Additionally, it achieves the best average NMI and ARI across all standard-sized datasets. In terms of CO, LGBQPC ranks fifth among the 12 compared methods, highlighting a favorable balance between accuracy and efficiency. Figure 3 further confirms its effectiveness in handling complex manifold structures and non-uniform density distributions (particularly evident in datasets D5 and D7-D9).

Following the Friedman test outlined in Section IV-A, the results from Table III yield test statistics of $\tau_F = 20.31$ for

NMI and $\tau_F = 19.93$ for ARI. Since both values exceed the critical threshold $F_{0.05}(11, 407) = 1.81$, the differences among the 12 clustering algorithms are statistically significant at the 0.05 level. Furthermore, the Nemenyi test results for both NMI and ARI, as presented in Fig. 4, indicate that LGBQPC significantly outperforms eight of the compared clustering algorithms, particularly three GB-based algorithms: GBSC, GBDPC, and GBCT.

On the other hand, Table IV demonstrates that LGBQPC attains superior clustering performance on the large-scale datasets D39 and D40, ranking first and second, respectively. Simultaneously, it maintains acceptable computational efficiency ranking seventh and fifth among the nine scalable algorithms. These results suggest that LGBQPC is well-suited for large-scale data analysis.

In summary, LGBQPC achieves statistically significant improvements over GBDPC, establishing itself an efficient, effective, and scalable clustering method capable of reliably addressing datasets with complex manifold structures or non-uniform density distributions.

C. Parameter Analysis

This section systematically evaluates the performance of LGBQPC under varying parameter configurations. The experiments are conducted on four representative datasets (D32-D35). The penalty coefficient (λ) is varied from 0 to $0.3 \sqrt[3]{n}$ in increments of $0.01 \sqrt[3]{n}$, while the number of nearest neighbors (k) is adjusted from 1 to 20 in steps of 1. The experimental results are presented in Figs. 5 and 6, respectively. Specifically, Fig. 5 illustrates the number of generated GBs across different penalty coefficients, and Fig. 6 evaluates the clustering performance of LGBQPC under different parameter configurations using NMI.

As illustrated in Fig. 5, the number of generated GBs follows a consistent pattern across all selected datasets, decreasing monotonically as the penalty coefficient increases. This indicates that the number of generated GBs can be efficiently controlled within an acceptable range by tuning the penalty coefficient in GB-POJG+.

Furthermore, Fig. 6 reveals that the best performance of LGBQPC is consistently achieved when a non-zero penalty coefficient is set across all selected datasets. This observation highlights the importance of integrating a penalty coefficient into the objective function of GB-POJG+. These findings suggest that generating GBs at coarser granularity, rather than

TABLE III
EXPERIMENTAL RESULTS ON DATASETS D1-D38

Criteria	Datasets	k -means++	SC	DBSCAN	DPC	DPC-DLP	FHC-LDP	USPEC	USENC	GBDPC	GBSC	GBCT	LGBQPC (Ours)
NMI (\uparrow)	D1	39.26 (9.0)	33.70 (10.0)	83.13 (5.0)	96.34 (3.0)	79.35 (6.0)	100.00 (1.5)	2.42 (12.0)	76.42 (7.0)	26.00 (11.0)	44.72 (8.0)	93.59 (4.0)	100.00 (1.5)
	D2	58.17 (12.0)	100.00 (3.5)	100.00 (3.5)	100.00 (3.5)	89.57 (7.0)	100.00 (3.5)	100.00 (3.5)	78.19 (9.0)	65.20 (11.0)	78.19 (9.0)	80.71 (8.0)	100.00 (3.5)
	D3	16.24 (12.0)	100.00 (2.5)	100.00 (2.5)	43.32 (9.0)	69.78 (7.0)	100.00 (2.5)	84.06 (5.0)	66.45 (8.0)	17.96 (11.0)	76.54 (6.0)	22.97 (10.0)	100.00 (2.5)
	D4	0.07 (12.0)	56.23 (7.0)	100.00 (3.0)	86.05 (6.0)	27.46 (8.0)	100.00 (3.0)	100.00 (3.0)	100.00 (3.0)	3.92 (10.0)	0.13 (11.0)	8.86 (9.0)	100.00 (3.0)
	D5	50.29 (8.0)	53.65 (7.0)	84.35 (5.0)	100.00 (2.5)	33.33 (12.0)	100.00 (2.5)	83.39 (6.0)	44.93 (9.0)	43.67 (10.0)	37.94 (11.0)	100.00 (2.5)	100.00 (2.5)
	D6	0.00 (12.0)	100.00 (3.5)	100.00 (3.5)	25.50 (10.0)	35.10 (9.0)	100.00 (3.5)	100.00 (3.5)	95.44 (7.0)	2.13 (11.0)	100.00 (3.5)	37.34 (8.0)	100.00 (3.5)
	D7	69.90 (9.0)	73.90 (8.0)	77.09 (6.0)	88.15 (3.0)	63.81 (12.0)	91.01 (2.0)	80.21 (5.0)	68.05 (10.0)	63.83 (11.0)	75.42 (7.0)	87.17 (4.0)	98.23 (1.0)
	D8	26.81 (8.0)	100.00 (3.0)	100.00 (3.0)	43.18 (7.0)	17.87 (9.0)	100.00 (3.0)	100.00 (3.0)	96.17 (6.0)	13.40 (10.0)	0.00 (12.0)	0.37 (11.0)	100.00 (3.0)
	D9	82.11 (8.0)	98.74 (4.0)	85.95 (7.0)	99.30 (2.5)	68.41 (10.0)	99.30 (2.5)	61.59 (12.0)	90.96 (6.0)	62.71 (11.0)	98.24 (5.0)	78.60 (9.0)	100.00 (1.0)
	D10	57.30 (11.0)	100.00 (3.0)	100.00 (3.0)	70.35 (10.0)	71.98 (9.0)	100.00 (3.0)	77.09 (6.0)	96.10 (7.0)	52.50 (12.0)	92.06 (8.0)	100.00 (3.0)	100.00 (3.0)
	D11	19.75 (12.0)	100.00 (4.0)	100.00 (4.0)	33.22 (10.0)	100.00 (4.0)	100.00 (4.0)	70.25 (8.0)	50.93 (9.0)	24.38 (11.0)	100.00 (4.0)	100.00 (4.0)	100.00 (4.0)
	D12	51.98 (12.0)	100.00 (3.5)	100.00 (3.5)	76.66 (9.0)	81.97 (8.0)	100.00 (3.5)	100.00 (3.5)	95.43 (7.0)	58.54 (11.0)	100.00 (3.5)	60.72 (10.0)	100.00 (3.5)
	D13	36.36 (11.0)	71.86 (7.0)	100.00 (2.0)	98.12 (5.0)	41.64 (10.0)	100.00 (2.0)	85.04 (6.0)	56.56 (9.0)	24.34 (12.0)	63.15 (8.0)	98.96 (4.0)	100.00 (2.0)
	D14	7.76 (12.0)	100.00 (3.5)	100.00 (3.5)	47.08 (9.0)	100.00 (3.5)	100.00 (3.5)	56.44 (7.0)	33.76 (10.0)	18.21 (11.0)	100.00 (3.5)	52.21 (8.0)	100.00 (3.5)
	D15	62.57 (12.0)	100.00 (3.0)	100.00 (3.0)	84.88 (8.0)	73.48 (10.0)	100.00 (3.0)	100.00 (3.0)	97.35 (6.0)	64.63 (11.0)	95.07 (7.0)	80.01 (9.0)	100.00 (3.0)
	D16	52.74 (8.0)	75.00 (7.0)	100.00 (3.0)	85.74 (6.0)	35.58 (10.0)	100.00 (3.0)	100.00 (3.0)	100.00 (3.0)	15.92 (11.0)	0.00 (12.0)	42.06 (9.0)	100.00 (3.0)
	D17	0.00 (12.0)	100.00 (3.5)	100.00 (3.5)	83.76 (7.0)	40.51 (10.0)	100.00 (3.5)	100.00 (3.5)	100.00 (3.5)	3.18 (11.0)	40.58 (9.0)	52.80 (8.0)	100.00 (3.5)
	D18	0.00 (12.0)	100.00 (5.5)	18.50 (11.0)	100.00 (5.5)	100.00 (5.5)	100.00 (5.5)	100.00 (5.5)					
	D19	0.88 (12.0)	23.60 (6.0)	20.22 (7.0)	30.30 (2.0)	15.87 (8.0)	30.03 (3.0)	5.42 (10.0)	2.66 (11.0)	12.42 (9.0)	26.53 (4.0)	25.47 (5.0)	79.61 (1.0)
	D20	35.71 (11.0)	100.00 (4.5)	67.47 (9.0)	45.42 (10.0)	18.96 (12.0)	100.00 (4.5)	100.00 (4.5)	100.00 (4.5)				
	D21	2.70 (12.0)	100.00 (4.0)	100.00 (4.0)	100.00 (4.0)	10.81 (10.0)	100.00 (4.0)	100.00 (4.0)	100.00 (4.0)	4.11 (11.0)	30.07 (8.0)	13.17 (9.0)	100.00 (4.0)
	D22	0.11 (11.0)	100.00 (3.5)	100.00 (3.5)	49.36 (9.0)	100.00 (3.5)	100.00 (3.5)	77.79 (8.0)	93.87 (7.0)	11.20 (10.0)	100.00 (3.5)	0.05 (12.0)	100.00 (3.5)
	D23	62.58 (11.0)	92.92 (3.0)	89.06 (5.0)	86.02 (7.0)	63.26 (10.0)	100.00 (1.5)	92.60 (4.0)	88.72 (6.0)	61.94 (12.0)	79.68 (8.0)	70.57 (9.0)	100.00 (1.5)
	D24	32.48 (11.0)	100.00 (4.0)	100.00 (4.0)	55.70 (9.0)	100.00 (4.0)	100.00 (4.0)	100.00 (4.0)	99.76 (8.0)	27.88 (12.0)	100.00 (4.0)	55.52 (10.0)	100.00 (4.0)
	D25	33.76 (1.0)	9.68 (8.0)	4.09 (11.0)	27.76 (3.0)	17.75 (4.0)	14.44 (5.0)	8.27 (10.0)	8.78 (9.0)	11.88 (6.0)	11.87 (7.0)	0.00 (12.0)	32.79 (2.0)
	D26	32.03 (2.0)	3.57 (10.0)	26.65 (3.0)	14.25 (5.0)	16.27 (4.0)	6.86 (8.0)	2.47 (11.0)	12.29 (7.0)	4.65 (9.0)	12.60 (6.0)	0.00 (12.0)	34.91 (1.0)
	D27	64.00 (9.0)	65.07 (7.0)	73.37 (5.0)	77.44 (2.0)	64.91 (8.0)	88.51 (1.0)	66.09 (6.0)	58.76 (10.0)	54.96 (11.0)	75.93 (3.0)	0.00 (12.0)	74.90 (4.0)
	D28	0.12 (10.0)	4.23 (2.0)	1.08 (6.0)	4.23 (2.0)	0.00 (11.5)	2.13 (4.0)	0.27 (8.0)	0.15 (9.0)	0.36 (7.0)	1.50 (5.0)	0.00 (11.5)	4.23 (2.0)
	D29	1.69 (5.0)	0.99 (9.0)	1.88 (4.0)	8.10 (1.0)	0.67 (10.0)	6.34 (2.0)	0.48 (11.0)	1.64 (6.0)	1.12 (8.0)	1.14 (7.0)	0.00 (12.0)	2.57 (3.0)
	D30	31.01 (6.0)	30.37 (8.0)	35.36 (3.0)	41.57 (1.0)	17.75 (10.0)	32.99 (5.0)	16.52 (11.0)	35.27 (4.0)	28.72 (9.0)	30.97 (7.0)	0.00 (12.0)	37.55 (2.0)
	D31	21.19 (7.0)	23.43 (6.0)	13.09 (11.0)	25.96 (2.0)	13.61 (10.0)	25.81 (3.0)	25.28 (4.0)	27.08 (1.0)	19.77 (9.0)	20.12 (8.0)	0.00 (12.0)	23.73 (5.0)
	D32	0.94 (9.0)	1.23 (6.0)	1.28 (5.0)	1.94 (3.0)	2.55 (1.0)	1.38 (4.0)	1.00 (8.0)	0.67 (10.0)	0.47 (11.0)	1.22 (7.0)	0.00 (12.0)	2.31 (2.0)
	D33	0.70 (10.0)	1.81 (8.0)	3.55 (4.0)	7.82 (2.0)	3.11 (5.0)	0.69 (11.0)	0.58 (12.0)	2.78 (6.0)	1.07 (9.0)	2.08 (7.0)	9.67 (1.0)	7.31 (3.0)
	D34	12.91 (5.0)	1.10 (12.0)	23.31 (3.0)	31.87 (1.5)	7.36 (8.0)	18.91 (4.0)	12.34 (6.0)	5.71 (9.0)	12.08 (7.0)	1.30 (11.0)	11.27 (1.0)	31.87 (1.5)
	D35	16.36 (4.0)	0.09 (10.0)	8.86 (6.0)	17.37 (2.0)	9.22 (5.0)	6.13 (8.0)	0.09 (10.0)	17.11 (3.0)	6.34 (7.0)	0.09 (10.0)	0.00 (12.0)	17.65 (1.0)
	D36	0.40 (11.0)	0.06 (12.0)	5.13 (9.0)	5.80 (8.0)	20.04 (4.0)	1.83 (10.0)	20.17 (3.0)	43.38 (1.0)	12.93 (5.0)	35.47 (2.0)	7.41 (7.0)	12.91 (6.0)
	D37	96.30 (10.0)	100.00 (4.0)	100.00 (4.0)	99.78 (8.0)	70.14 (11.0)	100.00 (4.0)	100.00 (4.0)	100.00 (4.0)	96.89 (9.0)	100.00 (4.0)	49.49 (12.0)	100.00 (4.0)
	D38	0.15 (9.0)	0.02 (11.5)	19.84 (1.0)	1.54 (6.0)	2.53 (5.0)	8.54 (3.0)	0.14 (10.0)	0.56 (8.0)	0.59 (7.0)	0.02 (11.5)	5.44 (4.0)	11.43 (2.0)
Average	28.35 (9.42)	61.09 (5.97)	67.30 (4.54)	56.54 (5.21)	46.47 (7.54)	69.34 (3.88)	58.35 (6.62)	57.67 (6.79)	25.46 (9.92)	50.80 (6.88)	40.41 (8.34)	72.95 (2.88)	
ARI (\uparrow)	D1	42.27 (9.0)	24.47 (10.0)	89.73 (5.0)	98.32 (3.0)	85.38 (6.0)	100.00 (1.5)	1.28 (12.0)	77.72 (7.0)	21.86 (11.0)	42.69 (8.0)	96.67 (4.0)	100.00 (1.5)
	D2	47.13 (12.0)	100.00 (3.5)	100.00 (3.5)	100.00 (3.5)	91.79 (7.0)	100.00 (3.5)	100.00 (3.5)	72.50 (10.0)	55.82 (11.0)	74.80 (9.0)	75.65 (8.0)	100.00 (3.5)
	D3	5.37 (12.0)	100.00 (2.5)	100.00 (2.5)	30.16 (9.0)	56.51 (7.0)	100.00 (2.5)	77.45 (5.0)	55.48 (8.0)	7.05 (11.0)	69.80 (6.0)	14.58 (10.0)	100.00 (2.5)
	D4	-0.57 (12.0)	45.94 (7.0)	100.00 (3.0)	85.02 (6.0)	8.47 (8.0)	100.00 (3.0)	100.00 (3.0)	100.00 (3.0)	1.59 (10.0)	-0.48 (11.0)	2.87 (9.0)	100.00 (3.0)
	D5	54.11 (8.0)	56.12 (7.0)	93.81 (5.0)	100.00 (2.5)	26.07 (12.0)	100.00 (2.5)	86.65 (6.0)	37.90 (9.0)	34.42 (10.0)	30.64 (11.0)	100.00 (2.5)	100.00 (2.5)
	D6	-0.17 (12.0)	100.00 (3.5)	100.00 (3.5)	13.60 (10.0)	25.92 (9.0)	100.00 (3.5)	100.00 (3.5)	95.37 (7.0)	1.07 (11.0)	100.00 (3.5)	29.07 (8.0)	100.00 (3.5)
	D7	65.81 (10.0)	68.60 (9.0)	86.88 (5.0)	90.98 (3.0)	69.16 (8.0)	93.91 (2.0)	76.44 (6.0)	59.55 (11.0)	56.44 (12.0)	70.87 (7.0)	90.34 (4.0)	99.36 (1.0)
	D8	15.22 (8.0)	100.00 (3.0)	100.00 (3.0)	39.00 (7.0)	6.20 (10.0)	100.00 (3.0)	100.00 (3.0)	97.60 (6.0)	8.15 (9.0)	0.00 (12.0)	0.30 (11.0)	100.00 (3.0)
	D9	74.59 (9.0)	99.18 (4.0)	92.63 (7.0)	99.59 (2.5)	59.11 (10.0)	99.59 (2.5)	37.12 (12.0)	94.80 (6.0)	47.62 (11.0)	98.77 (5.0)	76.85 (8.0)	100.00 (1.0)
	D10	51.64 (11.0)	100.00 (3.0)	100.00 (3.0)	62.63 (10.0)	70.53 (9.0)	100.00 (3.0)	95.56 (7.0)	97.55 (6.0)	43.63 (12.0)	93.04 (8.0)	100.00 (3.0)	100.00 (3.0)
	D11	13.74 (12.0)	100.00 (4.0)	100.00 (4.0)	23.37 (10.0)	100.00 (4.0)	100.00 (4.0)	70.98 (8.0)	51.12 (9.0)	16.36 (11.0)	100.00 (4.0)	100.00 (4.0)	100.00 (4.0)
	D12	39.44 (12.0)	100.00 (3.5)	100.00 (3.5)	74.76 (8.0)	72.24 (9.0)	100.00 (3.5)	100.00 (3.5)	93.07 (7.0)	49.43 (11.0)	100.00 (3.5)	54.45 (10.0)	100.00 (3.5)
	D13	41.32 (10.0)	76.26 (7.0)	100.00 (2.0)	99.20 (5.0)	39.89 (11.0)	100.00 (2.0)	85.99 (6.0)	54.32 (9.0)	19.22 (12.0)	65.58 (8.0)	99.60 (4.0)	100.00 (2.0)
	D14	9.40 (12.0)	100.00 (3.5)	100.00 (3.5)	43.25 (9.0)	100.00 (3.5)	100.00 (3.5)	59.11 (7.0)	26.06 (10.0)	12.78 (11.0)	100.00 (3.5)	50.65 (8.0)	100.00 (3.5)
	D15	48.82 (12.0)	100.00 (3.0)	100.00 (3.0)	76.16 (8.0)	67.42 (10.0)	100.00 (3.0)	100.00 (3.0)	97.62 (6.0)	50.48 (11.0)	96.31 (7.0)	70.91 (9.0)	100.00 (3.0)
	D16	39.86 (8.0)	66.57 (7.0)	100.00 (3.0)	78.18 (6.0)	13.99 (10.0)	100.00 (3.0)	100.00 (3.0)	100.00 (3.0)	7.23 (11.0)	0.00 (12.0)	33.22 (9.0)	100.00 (3.0)
	D17	-0.30 (12.0)	100.00 (3.5)	100.00 (3.5)	70.84 (7.0)	27.13 (10.0)	100.00 (3.5)	100.00 (3.5)	100.00 (3.5)	1.33 (11.0)	33.14 (9.0)	38.77 (8.0)	100.00 (3.5)
	D18	-0.10 (12.0)	100.00 (5.5)	16.53 (11.0)	100.00 (5.5)	100.00 (5.5)	100.00 (5.5)						
	D19	0.75 (12.0)	11.37 (6.0)	2.17 (11.0)	19.66 (2.0)	4.89 (9.0)	19.30 (3.0)	6.72 (7.0)	2.38 (10.0)	5.99 (8.0)	15.00 (4.0)	13.79 (5.0)	84.62 (1.0)
	D20	27.33 (11.0)	100.00 (4.5)	69.91 (9.0)	37.91 (10.0)	1.31 (12.0)	100.00 (4.5)	100.00 (4.5)	100.00 (4.5)				
	D21	3.62 (12.0)	100.00 (4.0)	100.00 (4.0)	100.00 (4.0)	14.51 (10.0)	100.00 (4.0)	100.00 (4.0)	100.00 (4.0)	4.96 (11.0)	19.20 (8.0)	15.28 (9.0)	100.00 (4.0)
	D22	0.04 (11.0)	100.00 (3.5)	100.00 (3									

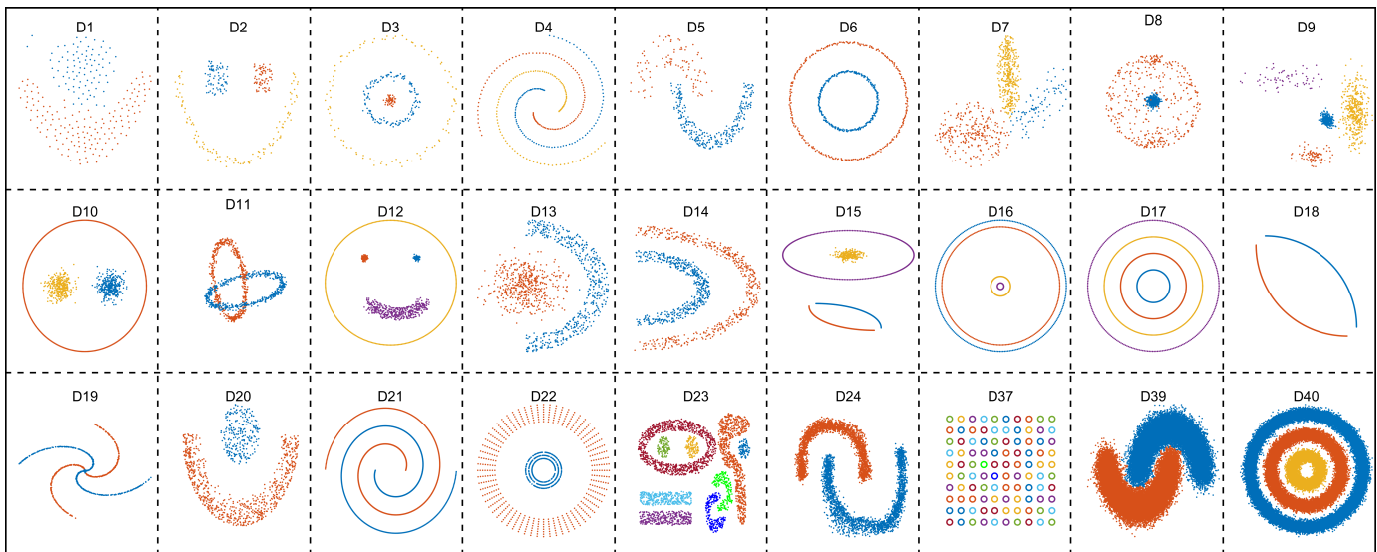


Fig. 3. Clustering results of LGBQPC on 27 synthetic datasets.

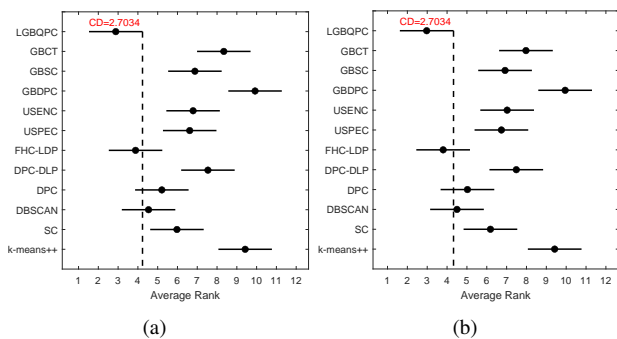


Fig. 4. Results of Nemenyi test on datasets D1-D38. (a) NMI. (b) ARI.

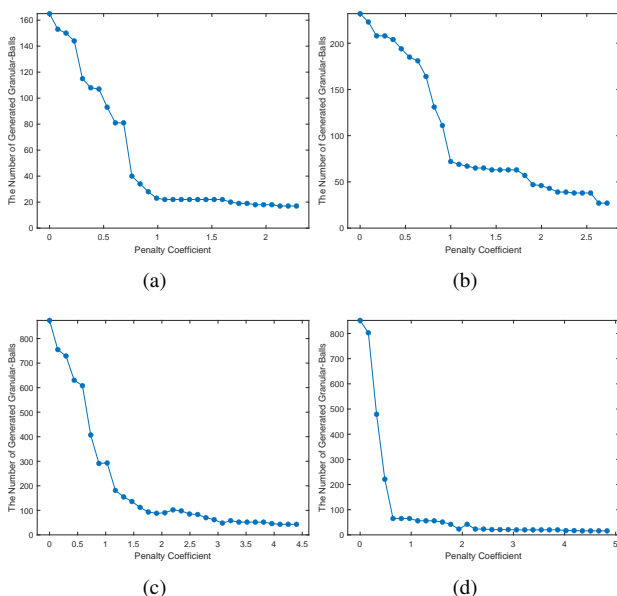


Fig. 5. Number of GBs generated by GB-POJG+ under varying penalty coefficients. (a)-(d) D32-D35.

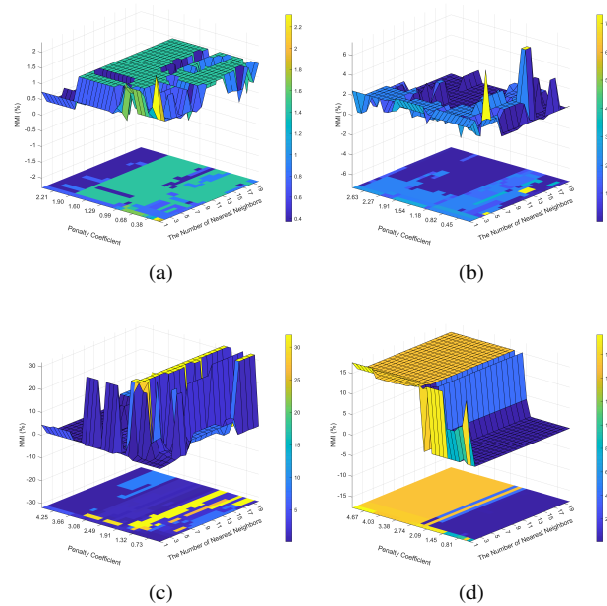


Fig. 6. Performance of LGBQPC under varying parameter configurations. (a)-(d) D32-D35.

- LGBQPC-v4: Identifies a GB as abnormal if it satisfies either the criteria from [15] or [20].
- LGBQPC-v5: Ensures each leaf node in the GB-based binary tree is sufficiently small but omits anomaly detection and subsequent complete division.
- LGBQPC-v6: Calculates GB density using Eq. (3).
- LGBQPC-v7: Estimates GB density based on Definition 2 and Eq. (9), without considering local structural information of GBs.
- LGBQPC-v8: Employs Eq. (4) as the distance metric for GBs, replacing the geodesic distance in Definition 11.

The experiments are performed on all datasets D1-D40. Notably, for each dataset, LGBQPC and its variants share the

same parameter settings, where the optimal configuration for LGBQPC is uniformly applied. The results are summarized in Table V. From Table V, the following insights can be drawn:

- (1) Comparing LGBQPC with its variants v1–v3 indicates that the definition of abnormal GBs presented in Definition 7 is more appropriate for LGBQPC than those proposed in [15], [18], [20]. Moreover, the performance of LGBQPC-v4 not only demonstrates the necessity of defining abnormal GBs using both average and maximum radii but also underscores the superiority of adaptive thresholds determined by mean and standard deviation over fixed ones.
- (2) The inferior results of LGBQPC-v5 demonstrate that the detection and complete division of abnormal leaf nodes during GB-based binary tree construction is essential for generating GBs with enhanced clustering suitability. In the other words, this mechanism effectively prevents the generation of GBs either located at decision boundaries or containing noise instances.
- (3) LGBQPC outperforms its variants v6 and v7, demonstrating that the relative quality metric in Definition 10 serves as a more effective density estimator for GBs. Avoiding density overestimation and incorporating local neighborhood information of GBs are two effective strategies for GB density estimation.
- (4) The experimental evaluation of LGBQPC-v8 reveals that adopting geodesic distance enhances LGBQPC’s ability to identify complex manifold structures, thereby effectively improving its clustering performance.

In summary, LGBQPC achieves superior clustering performance through effective improvements in: (1) abnormal GB definition, (2) GB-based binary tree construction, (3) GB density estimation, and (4) GB distance metric.

TABLE V
RESULTS OF ABLATION STUDIES ON DATASETS D1-D40

Algorithm	Average NMI (\uparrow)	Average ARI (\uparrow)	All CO (\downarrow)
LGBQPC (Ours)	74.22	74.08	9.59
LGBQPC-v1	58.45	55.86	4.73
LGBQPC-v2	64.11	62.42	7.69
LGBQPC-v3	58.23	54.11	20.75
LGBQPC-v4	67.75	66.22	7.55
LGBQPC-v5	59.12	56.6	5.03
LGBQPC-v6	61.58	59.78	10.98
LGBQPC-v7	68.57	67.15	10.04
LGBQPC-v8	26.17	19.45	8.55

V. CONCLUSION

This paper proposes a novel clustering algorithm, termed LGBQPC, which significantly improves the GBDPC algorithm through enhancements from both GB generation and clustering perspectives. Specifically, an advanced GB generation method, GB-POJG+, is developed building upon the GB-POJG framework. The proposed GB-POJG+ requires only a single parameter, namely the penalty coefficient, to ensure the generation of high-quality GBs while keeping their quantity within an acceptable range. Furthermore, to address the limitations of GBDPC in handling non-uniform density distributions and complex manifold structures, two key innovations are introduced based on the GB k -NN graph: (1) the use of relative

quality as an enhanced GB density estimator, and (2) the adoption of geodesic distance as an improved GB distance metric. These contributions collectively establish LGBQPC as an efficient, effective, and scalable clustering algorithm.

In future work, given the challenges of applying current GB computing methods to handling high-dimensional data [20], it is worthwhile to further investigate enhanced GB generation strategies and develop corresponding clustering methods for unlabeled high-dimensional data. Additionally, exploring effective strategies to automatically determine the optimal number of nearest neighbors for GBs in LGBQPC may offer further improvements in clustering performance [44].

REFERENCES

- [1] R. Xu and D. C. Wunsch, “Survey of clustering algorithms,” *IEEE Transactions on Neural Networks*, vol. 16, no. 3, pp. 645–678, 2005.
- [2] D. Arthur and S. Vassilvitskii, “K-means++: The advantages of careful seeding,” in *Proceedings of the 18th Annual ACM-SIAM Symposium on Discrete Algorithms*, 2007, pp. 1027 – 1035.
- [3] U. Von Luxburg, “A tutorial on spectral clustering,” *Statistics and Computing*, vol. 17, no. 4, pp. 395 – 416, 2007.
- [4] M. Ester, H. P. Kriegel, J. Sander, and X. Xu, “A density-based algorithm for discovering clusters a density-based algorithm for discovering clusters in large spatial databases with noise,” in *Proceedings of the 2nd International Conference on Knowledge Discovery and Data Mining (KDD)*, 1996, pp. 226–231.
- [5] A. Rodriguez and A. Laio, “Clustering by fast search and find of density peaks,” *Science*, vol. 344, no. 6191, pp. 1492–1496, 2014.
- [6] Y. Wang, J. Qian, M. Hassan, X. Zhang, T. Zhang, C. Yang, X. Zhou, and F. Jia, “Density peak clustering algorithms: A review on the decade 2014-2023,” *Expert Systems with Applications*, vol. 238, 2024, Art. no. 121860.
- [7] J. Hou and A. Zhang, “Enhancing density peak clustering via density normalization,” *IEEE Transactions on Industrial Informatics*, vol. 16, no. 4, pp. 2477–2485, 2020.
- [8] X. Fang, Z. Xu, H. Ji, B. Wang, and Z. Huang, “A grid-based density peaks clustering algorithm,” *IEEE Transactions on Industrial Informatics*, vol. 19, no. 4, pp. 5476–5484, 2023.
- [9] W. Tong, Y. Wang, and D. Liu, “An adaptive clustering algorithm based on local-density peaks for imbalanced data without parameters,” *IEEE Transactions on Knowledge and Data Engineering*, vol. 35, no. 4, pp. 3419–3432, 2023.
- [10] M. d’Errico, E. Facco, A. Laio, and A. Rodriguez, “Automatic topography of high-dimensional data sets by non-parametric density peak clustering,” *Information Sciences*, vol. 560, pp. 476–492, 2021.
- [11] M. Du, S. Ding, X. Xu, and Y. Xue, “Density peaks clustering using geodesic distances,” *International Journal of Machine Learning and Cybernetics*, vol. 9, pp. 1335–1349, 2017.
- [12] S. Ding, M. Du, T. Sun, X. Xu, and Y. Xue, “An entropy-based density peaks clustering algorithm for mixed type data employing fuzzy neighborhood,” *Knowledge-Based Systems*, vol. 133, pp. 294–313, 2017.
- [13] D. Cheng, Y. Li, S. Xia, G. Wang, J. Huang, and S. Zhang, “A fast granular-ball-based density peaks clustering algorithm for large-scale data,” *IEEE Transactions on Neural Networks and Learning Systems*, vol. 35, no. 12, pp. 17 202–17 215, 2024.
- [14] S. Xia, Y. Liu, X. Ding, G. Wang, H. Yu, and Y. Luo, “Granular ball computing classifiers for efficient, scalable and robust learning,” *Information Sciences*, vol. 483, pp. 136–152, 2019.
- [15] J. Xie, W. Kong, S. Xia, G. Wang, and X. Gao, “An efficient spectral clustering algorithm based on granular-ball,” *IEEE Transactions on Knowledge and Data Engineering*, vol. 35, no. 9, pp. 9743–9753, 2023.
- [16] D. Cheng, C. Zhang, Y. Li, S. Xia, G. Wang, J. Huang, S. Zhang, and J. Xie, “GB-DBSCAN: A fast granular-ball based DBSCAN clustering algorithm,” *Information Sciences*, vol. 674, 2024, Art. no. 120731.
- [17] S. Xia, B. Shi, Y. Wang, J. Xie, G. Wang, and X. Gao, “GBCT: Efficient and adaptive clustering via granular-ball computing for complex data,” *IEEE Transactions on Neural Networks and Learning Systems*, pp. 1–14, 2024. [Online]. Available: <http://doi.org/10.1109/TNNLS.2024.3497174>
- [18] J. Xie, M. Dai, S. Xia, J. Zhang, G. Wang, and X. Gao, “An efficient fuzzy stream clustering method based on granular-ball structure,” in *Proceedings of the IEEE 40th International Conference on Data Engineering (ICDE)*, 2024, pp. 901–913.

- [19] J. Xie, C. Hua, S. Xia, Y. Cheng, G. Wang, and X. Gao, "W-GBC: An adaptive weighted clustering method based on granular-ball structure," in *Proceedings of the IEEE 40th International Conference on Data Engineering (ICDE)*, 2024, pp. 914–925.
- [20] Z. Jia, Z. Zhang, and W. Pedrycz, "Generation of granular-balls for clustering based on the principle of justifiable granularity," *IEEE Transactions on Cybernetics*, vol. 55, no. 4, pp. 1687–1700, 2025.
- [21] J. Xie, X. Xiang, S. Xia, L. Jiang, G. Wang, and X. Gao, "MGNR: A multi-granularity neighbor relationship and its application in KNN classification and clustering methods," *IEEE Transactions on Pattern Analysis and Machine Intelligence*, vol. 46, no. 12, pp. 7956–7972, 2024.
- [22] Q. Xie, Q. Zhang, S. Xia, F. Zhao, C. Wu, G. Wang, and W. Ding, "GBG++: A fast and stable granular ball generation method for classification," *IEEE Transactions on Emerging Topics in Computational Intelligence*, vol. 8, no. 2, pp. 2022–2036, 2024.
- [23] S. Xia, X. Dai, G. Wang, X. Gao, and E. Giem, "An efficient and adaptive granular-ball generation method in classification problem," *IEEE Transactions on Neural Networks and Learning Systems*, vol. 35, no. 4, pp. 5319–5331, 2024.
- [24] M. Sajid, A. Quadir, and M. Tanveer, "GB-RVFL: Fusion of randomized neural network and granular ball computing," *Pattern Recognition*, vol. 159, 2025, Art. no. 111142.
- [25] J. Yang, Z. Liu, S. Xia, G. Wang, Q. Zhang, S. Li, and T. Xu, "3WC-GBNRS++: A novel three-way classifier with granular-ball neighborhood rough sets based on uncertainty," *IEEE Transactions on Fuzzy Systems*, vol. 32, no. 8, pp. 4376–4387, 2024.
- [26] L. Sun, H. Liang, W. Ding, and J. Xu, "Granular ball fuzzy neighborhood rough sets-based feature selection via multiobjective mayfly optimization," *IEEE Transactions on Fuzzy Systems*, vol. 32, no. 11, pp. 6112–6124, 2024.
- [27] W. Qian, Y. Li, Q. Ye, S. Xia, J. Huang, and W. Ding, "Confidence-induced granular partial label feature selection via dependency and similarity," *IEEE Transactions on Knowledge and Data Engineering*, vol. 36, no. 11, pp. 5797–5810, 2024.
- [28] S. Xia, S. Zheng, G. Wang, X. Gao, and B. Wang, "Granular ball sampling for noisy label classification or imbalanced classification," *IEEE Transactions on Neural Networks and Learning Systems*, vol. 34, no. 4, pp. 2144–2155, 2023.
- [29] C. Gao, X. Tan, J. Zhou, W. Ding, and W. Pedrycz, "Fuzzy granule density-based outlier detection with multi-scale granular balls," *IEEE Transactions on Knowledge and Data Engineering*, vol. 37, no. 3, pp. 1182–1197, 2025.
- [30] S. Cheng, X. Su, B. Chen, H. Chen, D. Peng, and Z. Yuan, "GBMOD: A granular-ball mean-shift outlier detector," *Pattern Recognition*, 2024, Art. no. 111115.
- [31] W. Pedrycz and W. Homenda, "Building the fundamentals of granular computing: A principle of justifiable granularity," *Applied Soft Computing*, vol. 13, no. 10, pp. 4209–4218, 2013.
- [32] W. Pedrycz, "Granular computing for machine learning: Pursuing new development horizons," *IEEE Transactions on Cybernetics*, vol. 55, no. 1, pp. 460–471, 2025.
- [33] R. Lande, "On comparing coefficients of variation," *Systematic Zoology*, vol. 26, no. 2, pp. 214–217, 1977.
- [34] S. M. Ross, *Introduction to Probability and Statistics for Engineers and Scientists*, 5th ed. San Diego, CA, USA: Elsevier, 2014.
- [35] G. Wang, "DGCC: Data-driven granular cognitive computing," *Granular Computing*, vol. 2, no. 4, pp. 343–355, 2017.
- [36] K. Bache and M. Lichman, "UCI machine learning repository," 2017, Datasets. [Online]. Available: <http://archive.ics.uci.edu/ml>
- [37] D. Huang, C. Wang, J. Wu, J. Lai, and C. Kwok, "Ultra-scalable spectral clustering and ensemble clustering," *IEEE Transactions on Knowledge and Data Engineering*, vol. 32, no. 6, pp. 1212–1226, 2020.
- [38] S. A. Seyedi, A. Lotfi, P. Moradi, and N. N. Qader, "Dynamic graph-based label propagation for density peaks clustering," *Expert Systems with Applications*, vol. 115, pp. 314–328, 2019.
- [39] J. Guan, S. Li, X. He, J. Zhu, and J. Chen, "Fast hierarchical clustering of local density peaks via an association degree transfer method," *Neurocomputing*, vol. 455, pp. 401–418, 2021.
- [40] J. Sander, M. Ester, H.-P. Kriegel, and X. Xu, "Density-based clustering in spatial databases: The algorithm GDBSCAN and its applications," *Data Mining and Knowledge Discovery*, vol. 2, no. 2, pp. 169–194, 1998.
- [41] S. Romano, J. Bailey, N. X. Vinh, and K. Verspoor, "Standardized mutual information for clustering comparisons: One step further in adjustment for chance," in *Proceedings of the 31st International Conference on Machine Learning (ICML)*, vol. 4, 2014, pp. 2873–2882.
- [42] M. Friedman, "A comparison of alternative tests of significance for the problem of m rankings," *Annals of Mathematical Statistics*, vol. 11, pp. 86–92, 1940.
- [43] O. J. Dunn, "Multiple comparisons among means," *Journal of the American Statistical Association*, vol. 56, pp. 52–64, 1961.
- [44] Q. Zhu, J. Feng, and J. Huang, "Natural neighbor: A self-adaptive neighborhood method without parameter K ," *Pattern Recognition Letters*, vol. 80, pp. 30–36, 2016.